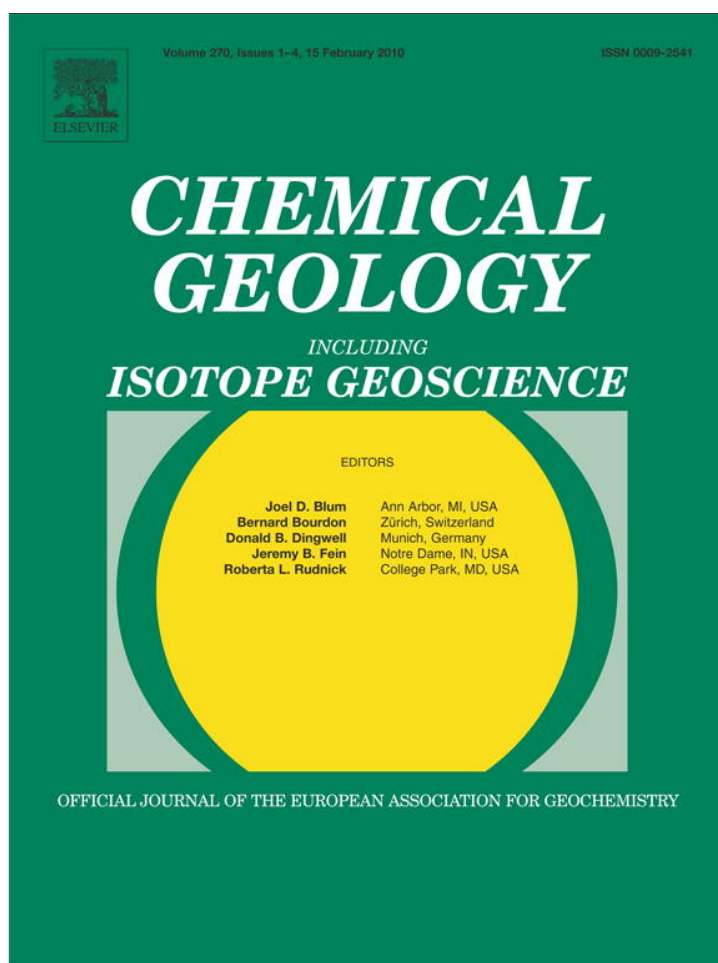


Provided for non-commercial research and education use.  
Not for reproduction, distribution or commercial use.



This article appeared in a journal published by Elsevier. The attached copy is furnished to the author for internal non-commercial research and education use, including for instruction at the authors institution and sharing with colleagues.

Other uses, including reproduction and distribution, or selling or licensing copies, or posting to personal, institutional or third party websites are prohibited.

In most cases authors are permitted to post their version of the article (e.g. in Word or Tex form) to their personal website or institutional repository. Authors requiring further information regarding Elsevier's archiving and manuscript policies are encouraged to visit:

<http://www.elsevier.com/copyright>



Contents lists available at ScienceDirect

Chemical Geology

journal homepage: [www.elsevier.com/locate/chemgeo](http://www.elsevier.com/locate/chemgeo)

## Ion microprobe analysis of oxygen isotopes in garnets of complex chemistry

F. Zeb Page<sup>a,b,\*</sup>, Noriko T. Kita<sup>a</sup>, John W. Valley<sup>a</sup>

<sup>a</sup> *Wisc SIMS, Department of Geoscience, University of Wisconsin – Madison, 1215 W. Dayton St., Madison, WI, 53706, USA*

<sup>b</sup> *Department of Geology, Oberlin College, 52 W. Lorain St., Oberlin, OH 44074, USA*

### ARTICLE INFO

#### Article history:

Received 14 July 2009

Received in revised form 2 November 2009

Accepted 2 November 2009

Editor: R.L. Rudnick

#### Keywords:

Garnet

Oxygen isotopes

SIMS

Ion microprobe

Adirondack Mountains

Skarn

Diffusion

### ABSTRACT

Accurate ion microprobe analysis of oxygen isotope ratios in garnet is possible if appropriate standards are employed to correct for instrumental bias, a component of which depends on the cation chemistry of the analyzed mineral. In this study, 26 garnet standards (including 14 new standards) that span the compositional range of pyrope, almandine, grossular, spessartine, and andradite were analyzed repeatedly by ion microprobe to develop a new method of correcting for instrumental bias in garnets. All analyses were normalized to a single master garnet standard (UWG-2) before bias from cation composition was considered. Bias due to cation composition in garnet was found to correlate with grossular content in pyrope garnets and with andradite in ugrandite garnets. Bias is correlated with molar volume in garnets of all compositions in this study. Although this correlation is suitable as a correction scheme for bias, a more accurate correction scheme based on the grossular and andradite compositions of garnet is proposed. This method reproduces the bias of all but one standard to within a range of 0.4‰, an accuracy that is on the same order as the reproducibility ( $\pm 0.3\%$ , 2 S.D.) of the master garnet standard UWG-2, but that remains an independent source of error. The new correction scheme is used to successfully reproduce laser fluorination analyses along a traverse of a polymetamorphic, zoned skarn garnet from the Adirondack Mountains. While previous analyses were at the mm-scale, the new data resolve a gradient of  $\delta^{18}\text{O}$  of 2.1‰ over 16  $\mu\text{m}$ . If experimentally derived diffusion coefficients are correct, these new results show that granulite-facies metamorphism was significantly faster than previously assumed and the thermal peak was less than 5 Myr.

© 2009 Elsevier B.V. All rights reserved.

### 1. Introduction

Metamorphism in hydrothermal systems or skarns is often accompanied by radical shifts in fluid composition and temperature over short time scales (e.g., Taylor and O'Neil, 1977; Bowman, 1998). In response to these changes, garnets and other minerals may form oscillatory zoning patterns in their major and trace element chemistry (e.g., Yardley et al., 1991; Jamtveit et al., 1993) as well as their oxygen isotope ratios (e.g., Clechenko and Valley, 2003). These micro-scale chemical and isotopic variations can be used to reconstruct ancient metamorphic fluid regimes. In particular, the oxygen isotope ratio of metamorphic garnet is a powerful tracer of hydrothermal systems because of the strong isotopic contrast between meteoric and most magmatic fluids (Valley, 1986) and the ability of garnet to preserve these ratios because of slow intragranular diffusion (e.g., Coghlan, 1990; Lancaster et al., 2009). However, the scale of isotopic heterogeneity within skarn minerals is generally much smaller than the volume of material required for analysis by conventional methods. Because of this, skarn garnets are an excellent target for oxygen isotope analysis by ion microprobe, and two studies have used single-collector ion microprobes to show that garnets

preserve a detailed oxygen isotopic record of hydrothermal fluid history (Jamtveit and Hervig, 1994; Crowe et al., 2001).

The most recent generation of multicollector ion microprobes has allowed significant advances for in situ oxygen isotope analysis both in terms of reduced analysis spot size and in analytical precision. Analyses of minerals with limited cation solid solution, such as zircon and quartz, have improved from  $\pm 2\%$  (2 S.D.) on 30  $\mu\text{m}$  diameter pits (e.g., Valley and Graham, 1991) to  $\pm 0.7\%$  (2 S.D.) on 20  $\mu\text{m}$  pits (Cavosie et al., 2005) to  $\pm 0.3\%$  (2 S.D.) on 10  $\mu\text{m}$  pits (Kelly et al., 2007; Kita et al., 2009; Valley and Kita, 2009). For ultra-small spots (<1  $\mu\text{m}$  in diameter) Page et al. (2007) attained a precision of  $\pm 2\%$  (2 S.D.). The smaller spot sizes and better precision can be attributed to improvements in technology and to refinements in technique, which include tuning and operation of the instrument, sample preparation, and standardization (Kita et al., 2009; Valley and Kita, 2009). For some minerals, including magnetite and hematite, the orientation of the crystal lattice has been shown to affect the instrument bias (Huberty et al., 2009), however, the data reported here show that any such orientation effect is smaller than the grain-to-grain precision of  $\pm 0.3\%$  that is regularly attained for randomly orientated grains of garnet. Due to the significant instrument bias inherent in ion microprobe analysis (e.g., Shimizu and Hart, 1982; Gnaser, 2008), accurate measurements of stable isotope ratios must be empirically corrected by regular and frequent analysis of well-characterized reference material. Because variable cation composition of some minerals or glasses

\* Corresponding author. Department of Geology, Oberlin College, 52 W. Lorain St., Oberlin, OH 44074, USA. Tel.: +1 440 775 6701; fax: +1 440 775 8038.  
E-mail address: [zeb.page@oberlin.edu](mailto:zeb.page@oberlin.edu) (F.Z. Page).

contributes to the instrumental bias (the “matrix effect” or instrumental mass fractionation e.g., Eiler et al., 1997; Valley and Kita, 2009), most ion microprobe studies of oxygen isotope ratios have been confined to phases of limited solid solution (e.g., zircon, quartz, calcite). In addition, many papers that address instrumental bias and propose correction schemes were developed for a previous generation of single-collector ion microprobes that made use of extreme energy filtering with only one collector and relatively low mass resolution (e.g., Hervig et al., 1992; Riciputi and Paterson, 1994; Eiler et al., 1997; Riciputi et al., 1998). Under these conditions, the instrumental bias can be in excess of 50‰ for  $\delta^{18}\text{O}$ . More recently, Vielzeuf et al. (2005a) addressed the issue of bias in a large-radius multicollector ion microprobe, specifically in aluminous  $\text{Fe}^{2+}$ -Mg-Ca garnets, and developed a new correction scheme to allow relatively accurate analyses of these compositions ( $\pm 1$ –2‰, 30–50  $\mu\text{m}$  pits). The instrument bias for these analyses at high mass-resolution (MRP~2500) and low energy offset was significantly lower, below 7‰. The cation compositional range of the standards introduced by Vielzeuf et al. (2005a) are sufficient to address the instrumental bias in Al-rich  $\text{Fe}^{2+}$ -Mg-Ca (pyralspite) garnets commonly found in metasedimentary, metamafic, and some igneous rocks. There are several studies that have established oxygen isotope zoning in garnets of these compositions (e.g., Kohn et al., 1993; Kohn and Valley, 1994; Kohn et al., 1997; Skelton et al., 2002; Peck and Valley, 2004) and some that have made use of ion microprobe analysis of zoned pyralspite garnets (Vielzeuf et al., 2005a,b; Martin et al., 2006; Lancaster et al., 2009). However, hydrothermal skarn garnets are most

commonly Ca-rich with variable  $\text{Fe}^{3+}/\text{Al}$  (ugrandite) and the Vielzeuf et al. (2005a) standard set and correction scheme does not extend to these compositions.

The present study uses new, higher precision analyses by the latest generation multicollector ion microprobe (ims-1280) to examine instrumental bias systematically from 26 garnet standards covering a wide range of solid solution, including more Ca-rich grossular and andradite compositions. This study has three main goals: 1) to increase the range of possible applications of this method; 2) to develop more straightforward, flexible and accurate correction schemes; and 3) to use these methods to evaluate the timing of metamorphic events or to place constraints on the rate of oxygen diffusion in garnet. We have applied our new correction procedure in the analysis of an oscillatory-zoned garnet from the Willsboro Mine, a polymetamorphosed garnet-diopside-wollastonite skarn from the Adirondack Mountains, New York, USA, described by Clechenko and Valley (2003).

## 2. Garnet standards

In this study, 27 garnets were used to evaluate matrix effects in oxygen isotope analysis by ion microprobe (Table 1). All of these standards were evaluated for oxygen isotopic homogeneity by ion microprobe, and for cation homogeneity by electron microprobe (Supplementary Table A). Oxygen isotope ratios were determined by laser fluorination for all new standards, and in some cases existing standards were analyzed as well for

**Table 1**  
Garnet standards analyzed for  $\delta^{18}\text{O}$  at WiscSIMS.

Standard	Average composition	Calculated molar V	2 S.D. <sup>a</sup>	$\delta^{18}\text{O}^b$ (‰ VSMOW)	Average <sup>c</sup> $\delta^{18}\text{O}^*$	Average bias % rel. UWG-2	2 S.D. <sup>d</sup>	$n^d$	2 S.E. <sup>d</sup>	Ref. <sup>e</sup>
<i>Pyrope</i>										
PypDM	Pyp <sub>97</sub> Alm <sub>3</sub>	113.2	0.07	5.60	4.42	−1.18	0.73	23	0.15	(6)
13-63-19	Pyp <sub>71</sub> Alm <sub>18</sub> Grs <sub>9</sub> Sps <sub>2</sub>	114.8	0.05	5.92	5.71	−0.21	0.29	10	0.09	(5)
PypAA	Pyp <sub>69</sub> Alm <sub>18</sub> Grs <sub>11</sub> Sps <sub>1</sub> Uv <sub>1</sub>	115.1	0.10	5.50	5.20	−0.30	0.25	10	0.08	(6)
PypAK	Pyp <sub>64</sub> Alm <sub>24</sub> Grs <sub>11</sub> Sps <sub>1</sub>	115.1	0.05	5.50	5.17	−0.33	0.42	10	0.13	(6)
PypMM	Pyp <sub>63</sub> Alm <sub>25</sub> Grs <sub>11</sub> Sps <sub>1</sub>	115.1	0.05	5.30	5.59	0.29	0.60	10	0.19	(6)
13-62-29	Pyp <sub>59</sub> Alm <sub>32</sub> Grs <sub>8</sub> Sps <sub>1</sub>	114.9	0.03	7.39	6.93	−0.46	0.56	10	0.18	(5)
13-62-27	Pyp <sub>49</sub> Alm <sub>35</sub> Grs <sub>15</sub> Sps <sub>1</sub>	115.9	0.06	6.49	6.66	0.17	0.36	10	0.11	(5)
13-63-20	Pyp <sub>48</sub> Alm <sub>31</sub> Grs <sub>20</sub> Sps <sub>1</sub>	116.5	0.12	6.14	6.85	0.71	0.34	10	0.11	(5)
13-63-44	Pyp <sub>45</sub> Alm <sub>29</sub> Grs <sub>25</sub> Sps <sub>1</sub>	117.0	0.12	6.37	7.06	0.69	0.53	10	0.17	(5)
<i>Almandine</i>										
AlmSE	Alm <sub>74</sub> Pyp <sub>25</sub> Grs <sub>1</sub>	114.9	0.03	8.30	7.13	−1.17	0.31	38	0.05	(2), (6)
AlmCMG	Alm <sub>70</sub> Pyp <sub>25</sub> Grs <sub>3</sub> Sps <sub>2</sub>	115.1	0.03	7.50	6.87	−0.63	0.65	14	0.17	(2), (6)
2B3	Alm <sub>67</sub> Grs <sub>24</sub> Sps <sub>4</sub> Pyp <sub>3</sub> And <sub>2</sub>	118.1	0.26	6.90	7.97	1.07	0.35	30	0.06	(6)
Beta114	Alm <sub>61</sub> Pyp <sub>31</sub> Grs <sub>6</sub> Sps <sub>2</sub>	115.3	0.09	9.30	8.55	−0.75	0.45	30	0.08	(6)
Bal509	Alm <sub>52</sub> Pyp <sub>44</sub> Grs <sub>3</sub> Sps <sub>1</sub>	114.7	0.04	12.30	11.31	−0.99	0.30	10	0.09	(6)
UWG-2	Alm <sub>45</sub> Pyp <sub>40</sub> Grs <sub>14</sub> Sps <sub>1</sub>	115.8	0.08	5.80	5.80	0.00	0.35	357	0.02	(1), (2), (6)
13-63-21	Alm <sub>41</sub> Grs <sub>31</sub> Pyp <sub>27</sub> Sps <sub>1</sub>	118.1	0.12	4.55	5.87	1.32	0.30	14	0.08	(5)
<i>Spessartine</i>										
SpsSE	Sps <sub>94</sub> Alm <sub>6</sub>	117.9	0.02	5.40	4.74	−0.66	0.36	19	0.08	(2), (6)
<i>Grossular</i>										
GrsSE	Grs <sub>94</sub> Alm <sub>4</sub> Sps <sub>1</sub> CaTi <sub>1</sub>	125.1	0.24	3.80	6.66	2.86	0.48	37	0.08	(2), (6)
92W-1	Grs <sub>87</sub> And <sub>5</sub> Alm <sub>5</sub> Pyp <sub>2</sub> CaTi <sub>1</sub>	125.2	0.42	−0.34	2.77	3.11	0.63	20	0.14	(4)
10691	Grs <sub>86</sub> And <sub>5</sub> Alm <sub>5</sub> Pyp <sub>2</sub> CaTi <sub>2</sub>	125.2	0.40	0.18	3.49	3.31	0.28	10	0.09	(4)
MexGrs	Grs <sub>86</sub> And <sub>8</sub> Pyp <sub>3</sub> Alm <sub>1</sub> Sps <sub>1</sub> CaTi <sub>1</sub>	125.5	0.47	10.60 <sup>f</sup>	16.05	5.45	0.67	22	0.14	(3)
AF749A	Grs <sub>81</sub> And <sub>10</sub> Alm <sub>5</sub> Pyp <sub>1</sub> Sps <sub>1</sub> CaTi <sub>2</sub>	125.5	0.26	−1.24	2.63	3.87	0.32	10	0.10	(4)
R-53	Grs <sub>61</sub> Alm <sub>19</sub> Pyp <sub>19</sub> CaTi <sub>1</sub>	121.2	0.14	5.33	7.85	2.52	0.15	5	0.07	(5)
<i>Andradite</i>										
92LEW2	And <sub>91</sub> Grs <sub>6</sub> Alm <sub>3</sub>	131.1	0.37	−1.47	5.63	7.10	0.78	10	0.25	(4)
92LEW7	And <sub>89</sub> Grs <sub>6</sub> Alm <sub>4</sub> Pyp <sub>1</sub>	131.0	0.33	−1.60	5.09	6.69	0.25	18	0.06	(4)
92LEW10	And <sub>50</sub> Grs <sub>42</sub> Alm <sub>4</sub> CaTi <sub>2</sub> Pyp <sub>2</sub>	128.4	0.28	−1.20	4.44	5.64	0.38	14	0.10	(4)
92LEW8	And <sub>49</sub> Grs <sub>43</sub> Alm <sub>4</sub> CaTi <sub>3</sub> Pyp <sub>1</sub>	128.4	0.34	−0.93	4.46	5.39	0.64	10	0.20	(4)

<sup>a</sup> ( $\text{cm}^3/\text{mol}$ ) calculated from compositional data, see text.

<sup>b</sup> Values of  $\delta^{18}\text{O}$  were calibrated against the VSMOW scale using UWG-2 by laser fluorination and gas-source mass spectrometry, see text.

<sup>c</sup> Average value measured by ion microprobe, corrected to UWG-2.

<sup>d</sup> Variability measured by ion probe.

<sup>e</sup> (1) Valley et al. (1995), (2) Eiler et al. (1997), (3) Riciputi et al. (1998), (4) Kohn and Valley (1998), (5) Schulze et al. (2003), (6) Vielzeuf et al. (2005a,b).

<sup>f</sup> Analysis includes inclusion material.

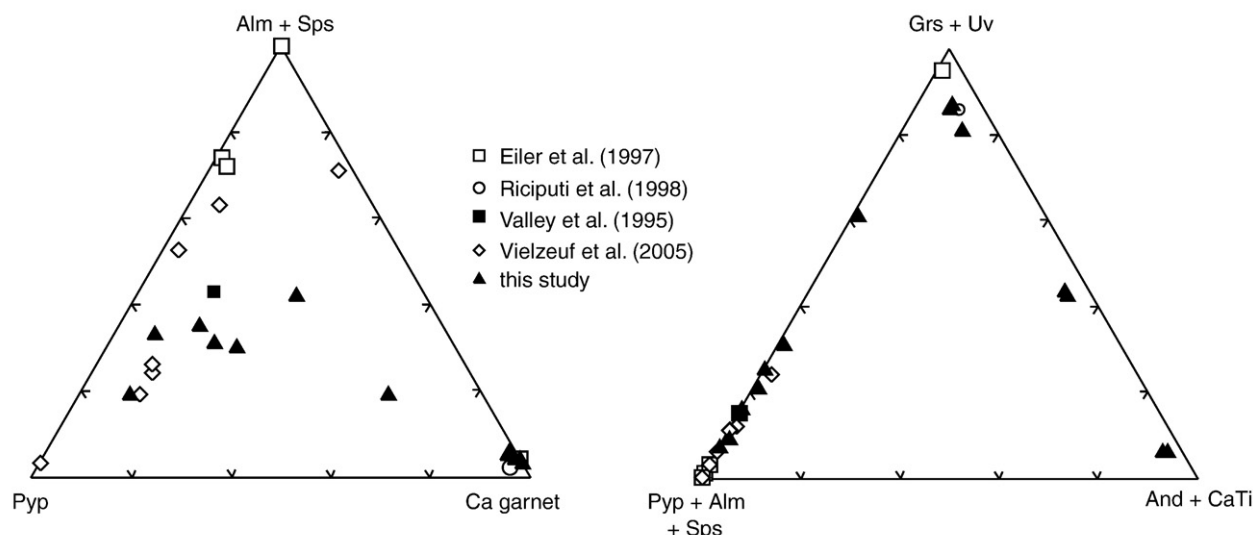


Fig. 1. Cation compositions of garnet standards used in this study. Standards are keyed to the study of their first use.

comparison to values in the literature. The standards used in this study and their average cation and isotopic compositions and observed isotopic variability are recorded in Table 1; cation compositions are shown in Fig. 1; electron microprobe analyses, cation variability and formula calculation are found in Table A, supplementary electronic materials.

Five garnet standards (Fig. 1) from Eiler et al. (1997) provide near-end-member compositions for grossular (GrsSE) and spessartine (SpsSE) garnets as well as slightly more dilute almandine (AlmSE & AlmCMG), and one intermediate almandine-pyrope (UWG-2) that is an extremely well-characterized standard for laser fluorination analysis of  $\delta^{18}\text{O}$  (Valley et al., 1995). Vielzeuf et al. (2005a) increased the cation compositional range of ion microprobe garnet standards, particularly along the pyrope-almandine join by including an end-member pyrope from the Dora Maira quartzite (PypDM) and five more intermediate compositions (PypMM, PypAk, PypAA, Bal509,  $\beta$ 114). In addition, they included one more standard on the almandine-grossular join (2B3). Detailed information on the origins of these standards as well as chemical composition and unit cell dimensions can be found in Vielzeuf et al. (2005a).

In addition to these existing standards, we introduce 6 garnet standards from eclogitic xenoliths in kimberlite with intermediate almandine-pyrope compositions and from 7 to 61 mol % grossular. Standards 13-63-21, 13-62-27, 13-62-29, 13-63-20, and 13-63-44 were separated by Dan Schulze from xenoliths found in the Blaauwbosch kimberlite, South Africa (Ford, 1987; Schulze et al., 2003). Standard R-53 is from an eclogitic xenolith found in the Roberts-Victor kimberlite (Garlick et al., 1971; MacGregor and Manton, 1986). To supplement the grossular-rich standard (GrsSE) used by both Eiler et al. (1997) and Vielzeuf et al. (2005a), we introduce three more grossular-rich garnets (92W-1, 10691, AF749A) from garnet-diopside-wollastonite skarn metamorphosed to the granulite facies (Willsboro-Lewis skarn belt, Adirondack Mts., Kohn and Valley, 1998). An additional grossular-rich sample, MexGrs (Riciputi et al., 1998) was also analyzed but was excluded from the standard set because of numerous inclusions. Finally, to investigate matrix effects on the grossular-andradite join, we include four more standards (92Lew-2, 92Lew-7, 92Lew-8, 92Lew-10) with the compositional range And<sub>49-91</sub>, from the same skarn belt (Kohn and Valley, 1998).

### 3. Analytical methods

#### 3.1. Sample preparation

Garnet standards were crushed by hand, cast in 25 mm epoxy disks, and polished. All garnet standards and samples were mounted within

5 mm of the center of the epoxy disk, and all mounts include multiple grains of the UWG-2 standard at the center of the mount. Standards vary in grain size from  $\sim 150\ \mu\text{m}$  to up to 5 mm, depending on the nature of the source material; between 3 and 36 grains of each standard were mounted in standard blocks. A zoned grossular-andradite garnet from the Willsboro wollastonite skarn (Adirondack Highlands, New York) that was previously analyzed for traverses of  $\delta^{18}\text{O}$  at mm-scale by laser fluorination (garnet 1a of Clechenko and Valley, 2003) using a thin saw-blade technique (Elsenheimer and Valley, 1993) was also prepared for ion microprobe analysis. The Willsboro sample consists of a 700  $\mu\text{m}$  thick polished wafer of rock (thick section) attached to a glass microscope slide with superglue from which a  $\sim 1\ \text{mm}$  wide strip of material that represents a core to rim garnet transect had been removed and analyzed in chips by laser fluorination. The portion of the garnet immediately adjacent to this transect was removed from the slide with acetone and cast in the center of an epoxy disk containing the UWG-2 standard and repolished for ion microprobe analysis.

#### 3.2. Electron microprobe

Cation chemistry of garnets was determined using the CAMECA SX51 electron microprobe at the University of Wisconsin – Madison. Garnets were analyzed in point beam mode with an accelerating potential of 15 kV and 20 nA beam current. The counting time was 10 s on peak and 5 s on both sides, off-peak. Natural and synthetic silicate and oxide standards were used. Data were reduced using the Probe for Windows software (Donovan et al., 2007), and oxygen was calculated by stoichiometry.  $\text{Fe}^{2+}/\text{Fe}^{3+}$  was estimated by charge-balance, assuming no site vacancies or OH substitution (Afifi and Essene, 1988). Chemical analyses of all garnet standards are presented in Supplementary Table A and summarized in Table 1.

#### 3.3. Laser fluorination

Analysis of oxygen isotopes to calibrate ion microprobe analyses for new standard material was performed on 1–2 mg garnet chips that were treated overnight at room temperature in the sample chamber with  $\text{BrF}_5$ , then individually heated with a  $\text{CO}_2$  laser in the presence of  $\text{BrF}_5$  to release  $\text{O}_2$ , which was cryogenically purified, converted into  $\text{CO}_2$ , and analyzed on a Finnigan MAT 251 mass spectrometer (Valley et al., 1995). Isotopic ratios are reported in permil (‰) notation relative to standard mean ocean water (VSMOW). Accuracy and analytical precisions were verified during each session by multiple

analyses of the garnet standard UWG-2 (Valley et al., 1995). Raw standard  $\delta^{18}\text{O}$  values for each session were corrected to the accepted UWG-2 value ( $\delta^{18}\text{O} = 5.80\%$  VSMOW) and the same correction was applied to samples. The average uncorrected  $\delta^{18}\text{O}$  value ( $\pm 2$  S.D.) of UWG-2 was  $5.59 \pm 0.08\%$  ( $n = 5$ ).

### 3.4. Ion microprobe

#### 3.4.1. Analysis conditions

Oxygen isotopic analyses were performed on the WiscSIMS CAMECA ims-1280 high-resolution, multi-collector ion microprobe at the University of Wisconsin – Madison in 10 analytical sessions over the course of over 2 years. A  $^{133}\text{Cs}^+$  primary ion beam (20 kV total accelerating voltage) was focused to a diameter of 10  $\mu\text{m}$  on the gold-coated sample surface. Secondary  $\text{O}^-$  ions were accelerated away from the sample by  $-10$  kV and the analysis site was centered under a uniform electron field generated by a normal-incidence electron gun for charge compensation. Primary ion intensities were ca. 2–3 nA. The secondary ion optics were configured similarly to those reported in Kita et al. (2009) in order to achieve high secondary ion transmission. Instrument parameters include: transfer lens magnification of 200, contrast aperture (CA) 400  $\mu\text{m}$  diameter, field aperture (FA)  $4000 \times 4000 \mu\text{m}$ , entrance slit width 122  $\mu\text{m}$ , energy slit width 40 eV, and exit slit width 500  $\mu\text{m}$ . At these conditions, both the primary ion spot image transferred to the FA window and the crossover image through the CA and entrance slit were almost fully transmitted compared to fully opened conditions. The intensity of  $^{16}\text{O}$  was 2 to  $3 \times 10^9$  cps depending on the primary intensity (ca.  $10^9$  cps/nA). Mass resolving power (MRP,  $M/\Delta M$ ), measured at 10% peak height, was set to ca. 2200, enough to separate hydride interferences on  $^{18}\text{O}$ . Two Faraday cups (FC) were used to measure  $^{16}\text{O}$  and  $^{18}\text{O}$  simultaneously and the amplifiers on each were equipped with  $10^{10}$  and  $10^{11} \Omega$  resistors, respectively. The base line of the FC amplifiers was measured at the beginning of each analytical session; drift during the day was insignificant compared to the noise level of the detectors ( $\leq 1000$  cps for the  $^{18}\text{O}$  FC with  $10^{11} \Omega$  resistor, Kita et al., 2009). The magnetic field was regulated by a Nuclear Magnetic Resonance (NMR) probe with stability of mass better than 10 ppm/10 h. At each analysis position, any small misalignment of the secondary optics due to changing stage position was automatically re-tuned before analysis. Instrument stability during each analytical session is documented by repeated analyses of the UWG-2 standard (Supplementary Table B).

#### 3.4.2. Standardization

Minerals with limited solid solution (e.g., quartz, calcite, zircon) are corrected for instrument bias by adjusting the raw data by a factor ( $\alpha^{18}\text{O}_{\text{SIMS}}$ ) obtained by analyzing a standard of the same mineral and chemical composition embedded in the same mount. Blocks of typically 4 standard analyses (different spots on one or more grains) are made before and after each set of sample analyses. In order to isolate the variation of bias generated by matrix effects within the garnet family from other sources of bias such as variability of instrument conditions over time, raw data from all garnet analyses (sample and compositional standard) were first corrected using the bracketing analyses of the UWG-2 standard that is embedded in each sample mount. A fractionation factor ( $\alpha^{18}\text{O}^*_{\text{SIMS}}$ ) is calculated from the bracketing analyses of UWG-2 relative to the accepted value of UWG-2 on the VSMOW scale (5.80‰, Valley et al., 1995) following equation 2.1 in Kita et al. (2009).

$$\alpha^{18}\text{O}^*_{\text{SIMS}} = \frac{1 + (\delta^{18}\text{O}_{\text{RAW}} / 1000)}{1 + (\delta^{18}\text{O}_{\text{VSMOW}} / 1000)} \quad (3.1)$$

A preliminary  $\delta^{18}\text{O}$  value for each sample (or compositional standard) is then calculated using  $\alpha^{18}\text{O}^*_{\text{SIMS}}$  and equation 2.5 of Kita et al. (2009).

$$\delta^{18}\text{O}^* = \left\{ \left[ 1 + (\delta^{18}\text{O}_{\text{RAW}} / 1000) \right] / \alpha^{18}\text{O}^*_{\text{SIMS}} - 1 \right\} \times 1000 \quad (3.2)$$

This preliminary corrected value is denoted as  $\delta^{18}\text{O}^*$  and is the same as  $\delta^{18}\text{O}_{\text{VSMOW}}$  only for garnets with the same bias (or chemical composition) as UWG-2 and  $\delta^{18}\text{O}^*$  increasingly differs from the VSMOW scale as garnet compositions (and biases) differ from that of UWG-2. The use of a preliminary correction to  $\delta^{18}\text{O}^*$  allows comparison of data between standard brackets or between different analysis sessions, but does not take into account the bias generated by chemical variability among garnets. This bias observed in the 25 other (secondary) garnet standards (vs. UWG-2) can be expressed in permil deviation from the bias observed in the analysis of UWG-2 with the following relation:

$$(\text{bias rel. UWG} - 2) \approx \delta^{18}\text{O}^* - \delta^{18}\text{O} \quad (3.3)$$

where  $\delta^{18}\text{O}$  is the isotopic composition of the standard on the VSMOW scale as determined by laser fluorination. Because the bias,  $\delta^{18}\text{O}^*$  and  $\delta^{18}\text{O}$  generally differ by less than 10‰ (and in most cases, they differ by much less) this approximation is accurate to within 0.1‰ (Kita et al., 2009).

For analyses of sample garnets, a correction is applied based on the compositional dependence of bias observed among standards analyzed during the same analysis session. Different possible correction schemes are compared in Section 5.4. In addition to isolating compositional effects from other sources of bias, this correction method allows us to use a single, particularly well-characterized standard (UWG-2) to evaluate spot-to-spot reproducibility of analyses by emulating the standard-sample-standard bracketing correction schemes used to ensure high precision and accuracy in oxygen isotopic analyses of other phases such as zircon, calcite, and quartz. Finally, using UWG-2 as a “master standard” allows a significant practical advantage in that only one standard need be embedded in each sample mount, and other standard material used to evaluate or correct for matrix bias can be reused in separate standard mounts as long as they are also corrected to UWG-2. The external errors of bracketing UWG-2 analyses were typically 0.2–0.4‰ (2 S.D.) for 10  $\mu\text{m}$  diameter analysis pits. After ion microprobe analysis, the bottoms of all pits were examined by scanning electron microscope in secondary electron imaging for inclusions and cracks that might affect the measured oxygen isotope ratios, and classified as “regular” or “irregular” according to Cavosie et al. (2005). All data used in this study are exclusively from pits that were observed to be “regular” (inclusion and crack-free).

#### 3.4.3. Sputter test

Eiler et al. (1997) observed a strong correlation with a single collector ion microprobe between the bias and sputter rate of glasses of various compositions and albite, and used this correlation as the foundation of a kinetic model to predict matrix effect bias. To compare the sputter rate of sample material with instrument bias, we conducted a sputtering rate test on a subset of garnet standards. The primary  $\text{Cs}^+$  ion beam was focused into a point beam and rastered over a  $30 \times 30 \mu\text{m}$  region for 60 min. The dimensions of the pits were measured at nm-scale using a Zygo white-light profilometer. The rastered pits were found to have flat bottoms, and the depth was taken as the average depth of the center portion of four transects through the center of each square pit. The reproducibility of this measurement was on the order of 2–3 nm for a single pit.

## 4. Results

Garnet standards were analyzed in ten sessions from April 2006 to August 2008, with between 3 and 25 standards analyzed per session. Each standard was analyzed between 4 and 20 times per session and bias data were corrected by the average bias calculated from the bracketing UWG-2 analyses. Instrumental bias measured on UWG-2 ranged from 1.5 to 4.6‰ between analysis sessions, but varied by less than 0.6‰ within a single session (average reproducibility =  $\pm 0.3\%$ ).



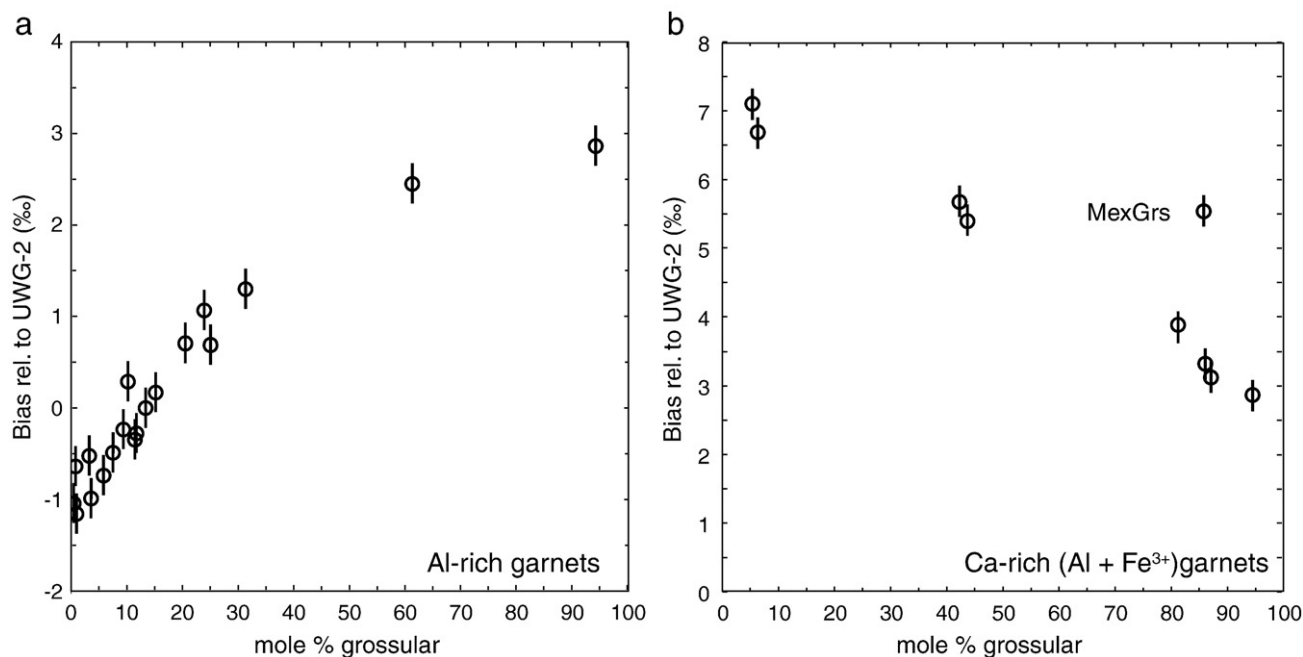


**Fig. 2.** Instrument bias for oxygen isotope analysis at WiscSIMS (‰ relative to UWG-2) as a function of cation composition of garnet standards expressed in terms of mol % garnet end-members. (a) Bias in Al-rich Mg-Fe<sup>2+</sup>-Ca-Mn garnets is correlated with grossular content (CaAl). (b) Bias in Ca-rich Al-Fe<sup>3+</sup> garnets is inversely correlated with grossular. MexGrs is poorly calibrated, see text.

analysis sessions include changes in instrumental conditions and may not be directly compared.

### 5.2. Bias and garnet composition

Instrument bias in garnets is strongly correlated with Ca-content in Al-rich garnets and appears to be approximately linear for compositions of less than ~30 mol% grossular (Fig. 2a). However, compositions of greater than 30 mol% grossular affect bias to a lesser degree. Bias changes ~2‰ relative to UWG-2 between 0 and 30 mol% grossular, but only increases an additional ~2‰ between 30 and 90 mol% grossular. This non-linear relationship between bias and composition is consistent with similar trends observed in feldspars, pyroxenes, olivine, and carbonates (Valley and Kita, 2009). In Ca-rich garnets, bias is inversely correlated with grossular (Al) content (Fig. 2b) and positively correlated with andradite (Fe<sup>3+</sup>), with one clear outlier (MexGrs). The instrumental bias measured for MexGrs is consistently 1‰ greater than the four other grossular-rich garnets of similar composition in this study. Ion microprobe analyses of MexGrs suggest that the garnet itself is not strongly variable in oxygen isotopic composition ( $\pm 0.7\%$ , 2 S.D.). However, unlike any other garnet in this study, MexGrs contains a substantial number of inclusions. Although these inclusions are easy to avoid with the ion microprobe, the calibration by laser fluorination analysis constitutes a mixture of garnet and inclusion material. For this reason we exclude MexGrs as a standard material in our calibration, although we show the data for completeness.

Vielzeuf et al. (2005a) recognized a correlation between the Ca content of Al-rich garnets and bias in most of their analysis sessions. This observation is largely based on one Ca-rich standard (GrsSE). The addition of more Ca-rich standards in this study confirms the strong correlation between Ca (grossular) and bias, and indicates that Fe<sup>+3</sup> (andradite) has an even stronger effect on instrumental bias.

### 5.3. Bias and molar volume

Andradite and grossular have a substantially larger unit cell dimension than the other garnet end-members in this study. In order to test a correlation between molar volume and instrument bias (a

possibility proposed by Vielzeuf et al., 2005a), the molar volume of each garnet standard was estimated as a weighted average of the molar volumes of end-members assuming ideal mixing. Volume data for pyrope, almandine, grossular, and andradite are taken from Robie and Hemingway (1995) and volume data for spessartine and uvarovite are from Diella et al. (2004). Physical properties of garnet such as unit cell dimension have long been successfully approximated from chemical data (e.g., Novak and Gibbs, 1971). The calculated molar volume for each standard can be found in Table 1, and agree well with the molar volumes determined for the subset of standards with published volumes determined by X-ray diffraction (Vielzeuf et al., 2005a).

The instrumental bias for the garnet standards in this study is well correlated with the calculated molar volume (Fig. 3). A least-squares linear regression of the data for all 26 standards (excluding MexGrs) yields an  $R^2$  value of 0.95. However, there is substantial variability of the data about the best-fit line, greater than the degree of observed heterogeneity in both cation and isotopic composition of the garnet standards. As in the study of Vielzeuf et al. (2005a), the lone spessartine-rich standard (SpsSE) lies well below the correlation between molar volume and bias line. However, SpsSE is not an outlier in the correlation between grossular and bias among Al-rich garnets (Fig. 2a).

Although the correlation between molar volume and bias provides a simple linear relationship, it does not explain the relatively large degree of variability observed among standards of similar cation composition, particularly those rich in grossular (even without MexGrs). One possibility in the case of greater observed bias than that predicted by calculated molar volume is the presence of an end-member such as hydrogrossular or hydroandradite that is analytically difficult to measure, but has a strong effect on molar volume. However, there is no evidence of a significant detectable hydrogen-bearing component (in the form of silica deficiency) for any of these standards. Although molar volume may provide a strong control on bias, one or more additional second-order effects may be responsible for the observed variability.

### 5.4. Correction scheme

Correlations between physical properties and instrumental bias have been reported before (Hervig et al., 1992; Eiler et al., 1997; Riciputi et al.,

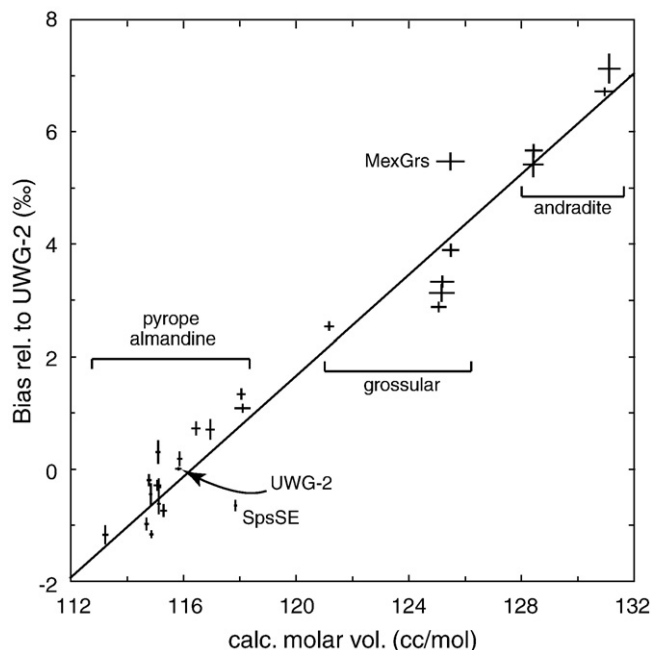


**Fig. 3.** Instrument bias for oxygen isotope analysis at WiscSIMS ( $\delta^{18}\text{O}$ , ‰ relative to UWG-2) as a function of calculated molar volume of the garnet standards. Errors are plotted as 2 S.E. The line is a least-squares linear regression (Eq. (5.1)) and yields an  $R^2$  value of 0.95. Two garnets (MexGrs and SpsSE) fall outside of 2 S.E. of the estimate.

1998). These workers noted a correlation between atomic mass and bias but also observed that the presence of residuals of up to 10‰ made this correlation unsuitable as a correction scheme. Most recently, Vielzeuf et al. (2005a) reported a correlation between molar volume and bias for garnets. However, because of limited standards, this correlation was deemed unsuitable as the basis for a correction scheme.

With the increased number of standards in this study, the observed correlation between calculated molar volume and bias could be used as a basis for correction. A least-squares linear regression of the data for 25 standards (not including the  $2\sigma$  outlier SpsSE) yields the relation:

$$\text{Bias}(\text{‰ relative to UWG} - 2) = 0.426 \times \text{calc. molar volume (cc/mol)} - 49.42 \quad (5.1)$$

with an  $R^2$  value of 0.97 (2 S.E. of the estimate = 0.88‰). This represents a substantial improvement in comparison to the correction scheme of Vielzeuf et al. (2005a) that was based on a linear interpolation of the bias of four standards that bracket the sample in almandine, pyrope, grossular, and spessartine content. The relation between bias and molar volume described by Eq. (5.1) reproduces the measured composition of 75% of the 25 standards used to within  $\pm 0.5\%$  of their accepted value, 85% to within  $\pm 0.6\%$ , and 95% to within 0.7%. Despite the extension in compositional range offered by this correction scheme, the improvement in accuracy ( $\pm 0.88\%$  2 S.E. of the estimate based on 25 garnets) is still substantially worse than the precision of the method as evidenced by typical reproducibility of standard analyses on the order of  $\pm 0.4\%$  (2 S.D.).

Another possible correction scheme is based on compositional variables, particularly the strong correlation between bias and grossular content in pyralpsite garnets and andradite in ugrandite garnets. Riciputi et al. (1998) showed that instrumental bias in grossular-andradite garnets in single-collector ion microprobes could be estimated using a linear interpolation of bias along the Al-Fe<sup>3+</sup> chemical join, and suggested that this be the basis of a correction scheme. In this study, the relationships between bias and grossular among pyralpsite garnets and between bias and andradite in ugrandite garnets are non-linear (Fig. 4). However, both are well-modeled with simple polynomial

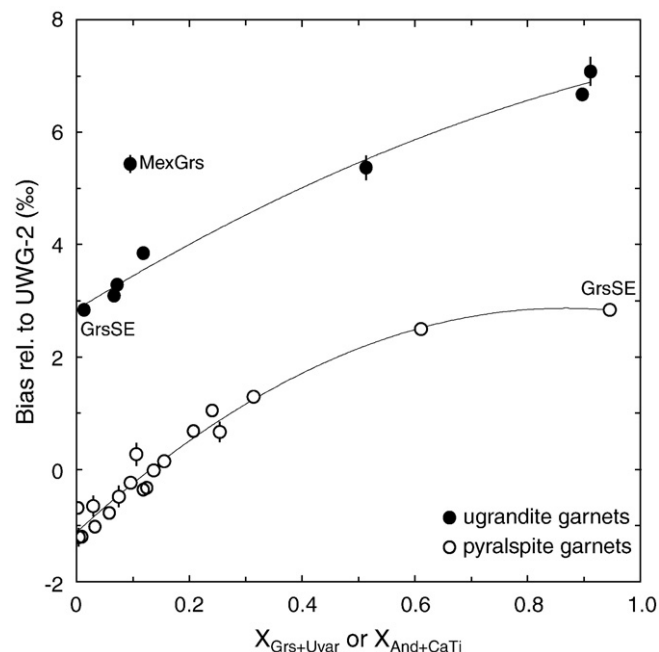


**Fig. 4.** Instrument bias for oxygen isotope analysis at WiscSIMS ( $\delta^{18}\text{O}$ , ‰ relative to UWG-2) as a function of Ca-rich garnet end-members. Instrumental bias in Al-rich pyralpsite garnets (plotted as open circles) increases with grossular + uvarovite content. Instrumental bias in Ca-rich ugrandite garnets (plotted as filled circles) is greater than that in pyralpsite garnets and increases with andradite + CaTi garnet content. Sample MexGrs is poorly calibrated, see text. Error bars are 2 S.E. of multiple analyses and are smaller than the sample points in most cases. The low-andradite grossular sample GrsSE appears in both plots. The polynomial best fit curves (Eqs. (5.2) and (5.3)) are also shown.

functions, with far less variability than the linear regression between molar volume and bias. This non-linear relationship is similar to that observed among other silicates and carbonates (Valley and Kita, 2009). The instrumental bias of the nineteen standards with less than 5 mol% andradite (including SpsSE) can be related to the mole fraction of grossular (+ minor uvarovite) with the following relation:

$$\text{Bias}(\text{‰ relative to UWG} - 2) = -5.04(X_{\text{Grs}+\text{Uvar}})^2 + 8.96(X_{\text{Grs}+\text{Uvar}}) - 1.09 \quad (5.2)$$

For the 8 garnet standards (excluding MexGrs) that contain less than 10% almandine + pyrope + grossular, bias can be related to andradite (+ minor CaTi garnet) as

$$\text{Bias}(\text{‰ relative to UWG} - 2) = -1.92(X_{\text{And}+\text{CaTi}})^2 + 6.18(X_{\text{And}+\text{CaTi}}) - 2.87 \quad (5.3)$$

These two calibrations reproduce the actual compositions of the 26 garnet standards used to  $\pm 0.40\%$  (2 S.E. of the estimate), a substantial improvement to the molar volume correction that makes accuracy comparable to the reproducibility of most garnet standards.

It is important to stress that the calibrations above are presented to demonstrate and compare between methods of correction. The values of instrumental bias measured relative to UWG-2 for each standard remain remarkably consistent between analysis sessions, but should in no way be the basis for correction of data collected on different instruments under different operating conditions. New calibration curves should be generated by users on their own instruments, ideally during the same analysis session as the samples to be corrected. The use of a calibration based on 26 garnet standards (or even a substantial subset thereof) that needs to be analyzed during each analysis session is impractical for routine correction of garnet data. A more practical

approach to a correction scheme correction is to use a subset of standards that compositionally bracket the unknown and then estimate bias based on the grossular or andradite composition as appropriate. Our preferred correction procedure is a calibration curve based on grossular or andradite composition. At least 3–4 standards are analyzed that bracket the chemical composition of the unknown sample and delineate the overall shape of the curve (e.g., both low and high grossular/andradite standards are included in each calibration to avoid artifacts that might arise from a quadratic equation fit to only three points over a narrow compositional range). Compositional standards should be analyzed during the same analysis session as samples to be corrected, if possible. A number of calibration curves were generated based on 3–4 standards using this approach. As long as the standards were chosen to cover a broad range of grossular or andradite compositions, the calibrations reproduced the full 26 garnet standard set to within  $\pm 0.3$ – $0.5\%$  (2 S.E. of the estimate). This approach yields similar accuracy to that achieved with use of all standards.

The use of a correction procedure in which all samples are first normalized to UWG-2 to correct for any instrumental instability and then corrected for matrix effect bias using the grossular or andradite of at least 3 secondary standards that compositionally bracket the unknown offers significant advantages in precision, accuracy, and convenience. Correction to a master standard allows for a single consistent method of determining the precision (reproducibility) of analyses as well as the practical advantage of allowing compositional standards to be stored in standard mounts and not embedded with samples. This allows use of the best and most plentiful standard for all sample mounts, and conserves more precious materials.

Errors in ion microprobe analyses arise from a myriad of sources ranging from counting statistics to sample topography (e.g., Kita et al., 2009). Propagation of all these sources of error would be an extremely arduous undertaking, and for this reason the external reproducibility of a standard is the best (and most workable) metric for error estimation (Valley and Kita, 2009). An instrumental bias calibration that is dependent on compositional variables introduces a new source of error independent of that measured by standard reproducibility. Errors resulting from the calibration scheme must therefore be added in quadrature to those arising from analytical uncertainty. However, it should be noted that the proposed calibration does not fully explain all sources of instrumental bias just as counting statistics do not encompass all other sources of error in an analysis. True statistical rigor in the treatment of these uncertainties is, as yet, impossible.

## 6. Application to growth zoning and diffusion

### 6.1. Adirondack skarn garnet

The Adirondack Mountains of New York, USA are a Mid-Proterozoic, polymetamorphic, granulite-facies orogenic terrane. Intrusion of anorthosite and related magmas ( $1155 \pm 5$  Ma, McLelland et al., 2004) formed a contact metamorphic aureole including skarn rocks that predate the peak of regional metamorphism (Valley and O'Neil, 1982; Valley, 1985; Valley et al., 1990). The Adirondack skarns were buried and largely recrystallized during the Ottawa (ca. 1050 Ma) regional granulite-facies metamorphism, but small domains of unrecrystallized, oscillatory-zoned skarn garnets were locally preserved at the Willsboro Mine. Clechenko and Valley (2003) analyzed the oxygen isotopic composition of one to two centimeter diameter zoned garnets from Willsboro by laser fluorination of mm-scale chips taken from a core to rim transect of the garnets removed with a thin diamond saw. The oxygen isotopic composition of this transect in combination with major and trace element data were used to infer variable mixing of metamorphic fluids from meteoric (low  $\delta^{18}\text{O}$ , Ca-rich) and magmatic (high  $\delta^{18}\text{O}$ , Fe-rich) sources. The garnet zoning was preserved through subsequent granulite-facies metamorphism.

In this study we analyze oxygen isotope ratios along a traverse in one of the garnets (garnet 1a) previously analyzed by Clechenko and Valley (2003) collected from the Willsboro Mine, NY, USA (approximately  $44^{\circ}18'52''\text{N}$ ,  $73^{\circ}52'54''\text{W}$ ) in order to assess the accuracy of our correction technique, as well as to search for finer-scale isotopic zoning and possibly larger variation than could be resolved by the existing analyses. The previous laser fluorination data document gradients in  $\delta^{18}\text{O}$  of  $\sim 3\%$  over 1 mm, but larger and sharper gradients are predicted for contact metamorphism. The new ion microprobe data interrogate these gradients at a scale that is up to 100 times finer in linear resolution and one million times smaller in volume.

### 6.2. Analysis and correction

The remainder of the polished section of garnet 1a of Clechenko and Valley (2003) was mounted in epoxy with standard UWG-2 and repolished. The original Fe–K $\alpha$  X-ray map of the composition of this garnet is reproduced in Fig. 5a with the location of the laser-fluorination traverse and the new ion microprobe traverse. The traverse in this study was located adjacent to and parallel with the previous traverse. Seventy ion microprobe analyses were performed along the 7.3 mm transect and corrected to the UWG-2 standard. The cation composition of the garnet was determined adjacent to each ion microprobe pit by electron microprobe, and used to correct the raw data for bias. The data were corrected using four grossular standards (GrsSE, 92W-1, 10691, AF749A) and two intermediate grossular–andradite standards (92LEW10, 92LEW7). The intermediate grossular–andradite standards were analyzed in the same analysis session as the zoned garnet (June 2007) and the four grossular standards were analyzed in a separate session (August 2008). Instrumental biases for both these sessions are reported in Table 2. 92LEW7 was analyzed during both analytical sessions, and its bias relative to UWG-2 differed by 0.03‰. Although analysis of secondary garnet standards during the same analysis session is desirable, normalization to UWG-2 allows this correction to be made with a negligible change in estimated precision and accuracy. Ion microprobe analyses of standards, cation compositions for each analysis point, and the correction scheme used are presented in Table D and Figure B, electronic supplementary materials.

### 6.3. Results and discussion

The andradite composition of garnet 1a is plotted vs. distance from the garnet rim in Fig. 5b. The overall pattern of chemical composition is almost identical to the traverse made by Clechenko and Valley (2003, see their Fig. 5a), but was offset ca. 300  $\mu\text{m}$  along strike of the banding. The oxygen isotopic traverse from this study is plotted in Fig. 5c, superimposed on the laser fluorination data of Clechenko and Valley (2003).

The oxygen isotope zoning in garnet 1a measured by ion microprobe is quite well correlated with that measured by laser fluorination. Two relatively andradite-rich, high- $\delta^{18}\text{O}$  zones are interspersed with andradite-poor, low- $\delta^{18}\text{O}$  zones within 7300  $\mu\text{m}$  of the rim (Fig. 5b). The ion microprobe analyses reproduce most of the laser fluorination traverse within the stated uncertainty of the technique. However, ion microprobe analyses of the outermost low- $\delta^{18}\text{O}$  zone yield isotope ratios up to 1‰ lower than that determined by the one laser fluorination analysis at 0–1000  $\mu\text{m}$ . Although it is possible that this discrepancy is due to a source of bias that is unaccounted for in the correction scheme, this seems unlikely, especially since there is no indication of a hydrogrossular component in this sample. Other intermediate grossular composition zones in this garnet show close agreement between laser and ion microprobe analyses (e.g., 4500  $\mu\text{m}$  from the rim), suggesting that no systematic relationship between grossular and analysis misfit exists. Mixed-

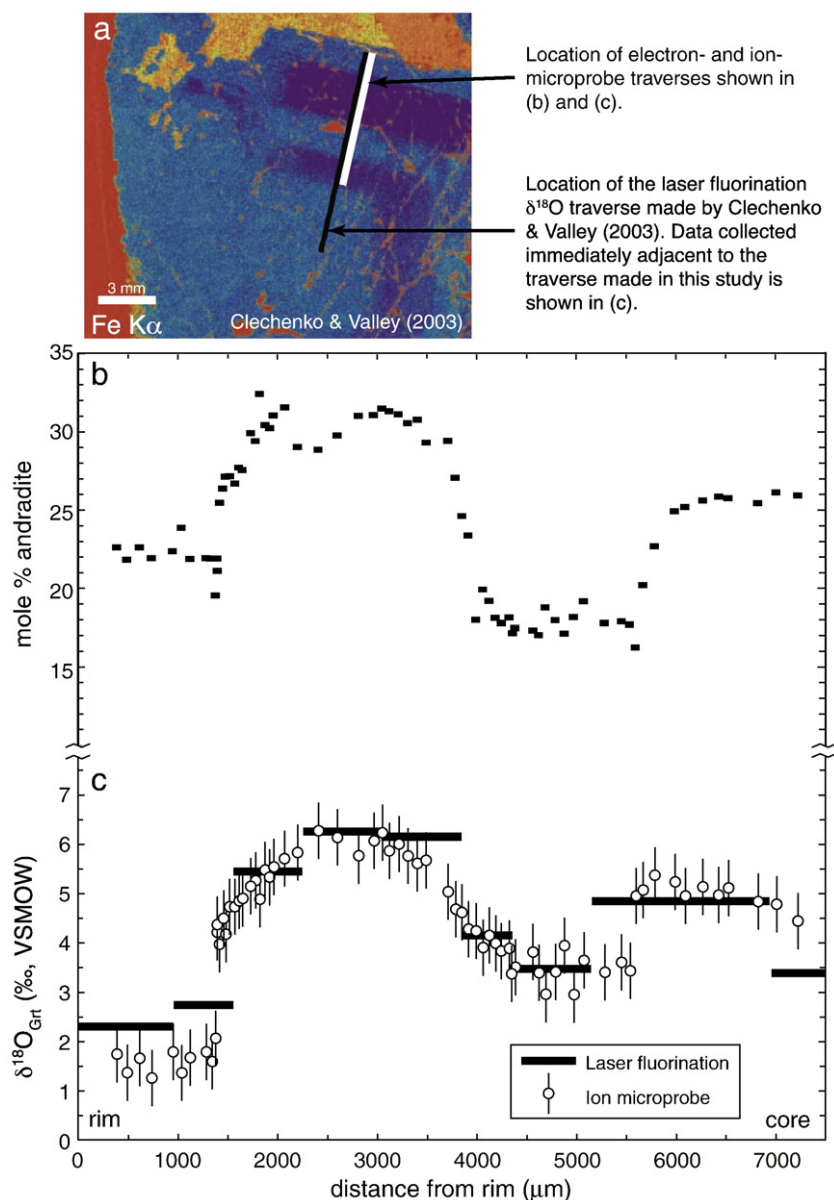


**Fig. 5.** Oscillatory-zoned skarn garnet from the granulite-facies Willsboro wollastonite skarn, Adirondack Mountains, New York, USA. (a) Fe-K $\alpha$  X-ray image of the garnet showing darker-shaded andradite-rich zones (purple in the web version of this article) and lighter-shaded grossular-rich zones (blue). Lighter colored minerals (yellow and orange in the web version) are sphene and feldspar. The location of the  $\delta^{18}\text{O}$  analyses by laser fluorination (Clechenko and Valley, 2003) are shown as a thick black line, the location of the ion microprobe traverse in this study is shown as a thick white line. (b) mol% andradite determined by electron microprobe vs. distance from garnet edge (top of figure). (c) traverses of  $\delta^{18}\text{O}$ , open symbols represent ion microprobe analyses with  $\pm 0.6\%$  error bars that represent both the precision ( $\pm 0.3\%$ ) and bias correction ( $\pm 0.4\%$ ) black bars are the laser fluorination data of mg-size samples by Clechenko and Valley (2003).

composition laser analyses are the most likely explanation for this discrepancy.

Examination of this and similar garnets from Willsboro and related nearby wollastonite skarns shows that the andradite bands parallel euhedral crystal faces of garnet (Clechenko and Valley, 2003). In many cases, zoning is preserved in only parts of the garnet. In Fig. 5a, these bands can be seen to become diffuse 3–5 mm to the left of the analysis traverses because the garnet was sheared and recrystallized during granulite facies metamorphism. Similar recrystallization has affected most of the garnets at Willsboro with the result that their cation compositions are homogenized and that they record Sm–Nd ages reset during regional metamorphism at ca. 1035 Ma (Basu et al., 1988). Taken together, all data support the interpretation that zoned garnets formed at the time of contact metamorphism and were locally preserved in low strain zones during recrystallization ca. 100 Myr later. The sharp chemical zonation that parallels garnet crystal faces

(Fig. 5a) resulted from growth zoning at 1155 Ma and is texturally and chemically distinct from the more diffuse effects of granulite facies recrystallization.

In the unrecrystallized domains of garnet 1a, BSE imaging and electron microprobe analyses reveal oscillatory zonation in Al and Fe $^{3+}$  but not the multiple  $\mu\text{m}$ -scale oscillations characteristic of many skarn garnets. Ion microprobe analysis of oxygen isotope ratios in this garnet reveals a generally smooth profile with only two sharp changes in isotopic composition ( $\sim 1400$  and  $\sim 5500$   $\mu\text{m}$  from the garnet edge). The absence of many  $\mu\text{m}$ -scale oscillatory features could be due to an initially smooth zoning profile, or could be due to diffusional relaxation of chemical and isotopic gradients during the granulite-facies regional metamorphic overprint. Clechenko and Valley (2003) calculated a characteristic length scale of diffusion (distance over which 50% exchange is predicted to have taken place) of 60  $\mu\text{m}$  for oxygen in the Willsboro garnets based on the experiments of

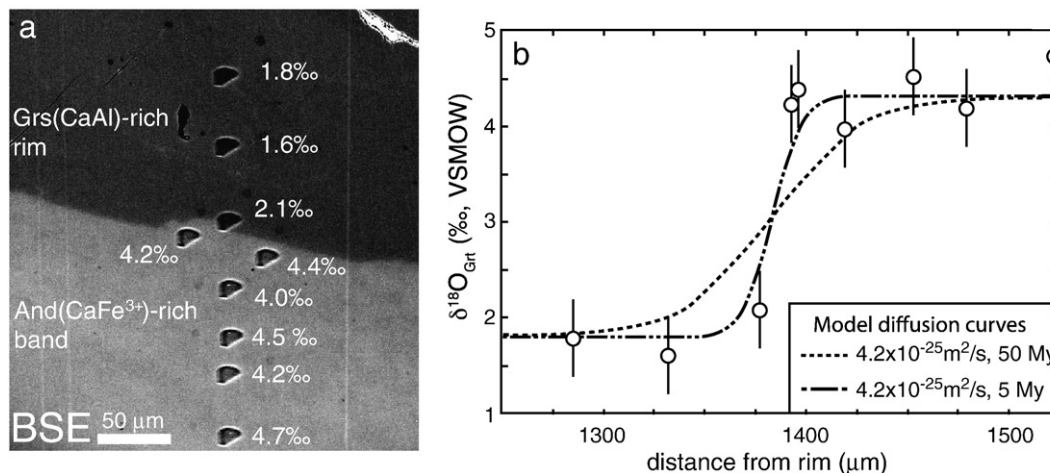


**Fig. 6.** Sharp  $\delta^{18}\text{O}$  and cation discontinuity 1377  $\mu\text{m}$  from the garnet edge (a) High-contrast back-scattered electron image of the sharp andradite-grossular transition within the garnet. Ion microprobe pits (10  $\mu\text{m}$  dia.) are labeled with  $\delta^{18}\text{O}$  ‰ VSMOW. (b) detail of  $\delta^{18}\text{O}$  traverse over the same field of view with simulated diffusion profiles (see text).

Coghlan (1990) and a thermal event of 750  $^{\circ}\text{C}$  for 50 My, based on regional thermobarometry and geochronology (Bohlen et al., 1985; McLelland et al., 2001). This length-scale of homogenization is consistent with the data-set of Clechenko and Valley (2003) and suggested that fine-scale chemical features were homogenized in the Willsboro garnets, and only mm-scale zonation was preserved through granulite-facies metamorphism.

The most important feature of the new ion microprobe data for  $\delta^{18}\text{O}$  is the sharp gradient between the outermost low- $\delta^{18}\text{O}$  rim and high- $\delta^{18}\text{O}$  zone between 1377 and 1393  $\mu\text{m}$  from the edge of the garnet (Fig. 5c). This transition represents a jump of 2.1‰ in 16  $\mu\text{m}$  (measured from the center of the analysis pits) coincident with an equally sharp change in the andradite content of garnet visible in the back-scattered electron image in Fig. 6a. Although  $\delta^{18}\text{O}$  decreases gradually across the Fe-rich band from a maximum of 6.3‰ at 2400  $\mu\text{m}$  to 4.2‰ at 1400  $\mu\text{m}$ , the oxygen isotope ratios measured in the outermost grossular-rich zone are constant at 1.8‰ (Fig. 5c). If the gradual decrease in  $\delta^{18}\text{O}$  within the more andradite-rich band were the result of diffusional relaxation after garnet growth across an original step-change in  $\delta^{18}\text{O}$  at 1380  $\mu\text{m}$ , a symmetrical increase in  $\delta^{18}\text{O}$  would occur in the adjacent grossular-rich zone approaching 1380  $\mu\text{m}$ . No gradual change is seen from 500 to 1380  $\mu\text{m}$  and thus the smooth changes in  $\delta^{18}\text{O}$  within the andradite-rich band are interpreted as growth-zoning, as is the sharp 2.1‰ gradient at 1380  $\mu\text{m}$  between these two zones.

The preservation of a sharp gradient in  $\delta^{18}\text{O}$  at 1380  $\mu\text{m}$  provides a very tight constraint on the maximum amount of oxygen diffusion in this garnet throughout its entire history. There is no diffusional process that would sharpen a  $\delta^{18}\text{O}$  gradient, once formed. Thus, the maximum amount of oxygen exchange can be estimated if the gradient is assumed to have formed as a step of 2.1‰ over 0  $\mu\text{m}$ . An equally sharp gradient in Al and  $\text{Fe}^{3+}$  is coincident with the oxygen discontinuity. This is a boundary condition, and it is possible that garnet growth produced a more gradual profile, closer to that observed in this garnet. If this were the case, models based on an initial step condition will over-estimate the duration of the metamorphic event or rate of exchange.

Diffusion of oxygen across this boundary was modeled as a simple, 1-dimensional system using equation 3.45 of Crank (1975). Because of the small scale of diffusion (<16  $\mu\text{m}$ ) compared to the size of the garnet (>1 cm), the 1-D model is a conservative approximation. Initial values for core and rim  $\delta^{18}\text{O}$  were taken as the average of ion microprobe data within 100  $\mu\text{m}$  of the transition ( $4.3 \pm 0.4\%$  and  $1.8 \pm 0.5\%$ , respectively). The sharp  $\text{Fe}^{3+}/\text{Al}$  and  $\delta^{18}\text{O}$  transition boundary at 1380  $\mu\text{m}$  is shown in back-scattered electron imaging in

Fig. 6a and analysis pits are labeled in  $\delta^{18}\text{O}$  VSMOW. A detail of the ion-microprobe traverse in this region is shown in Fig. 6b with modeled diffusion curves superimposed on the data. At 750  $^{\circ}\text{C}$ , the diffusion rate ( $D$ ) of oxygen in garnet based on the experiments of Coghlan (1990,  $P_{\text{H}_2\text{O}} = 1 \text{ kbar}$ ) is estimated at  $4.2 \times 10^{-25} \text{ m}^2 \text{ s}^{-1}$ . At this rate, the observed step could only have survived a thermal event of less than 1 My. Furthermore, this calculation does not include the effects of diffusion that would have also occurred during the heating and cooling of regional metamorphism. The extremely rapid heating and cooling required by the sharp gradient in this garnet interpreted in the context of the experiments of Coghlan (1990) are in striking contrast to the slow cooling rates of  $\sim 1.5$   $^{\circ}\text{C}/\text{My}$  reported by Mezger et al. (1991) for this region. Although fleeting thermal events have recently been proposed for regional metamorphism (e.g., Ague and Baxter, 2007), it seems unlikely that the mid-crustal, 7–8 kb granulite-facies regional metamorphism of the Adirondack Highlands could have taken place over so short a time span. Coghlan (1990) reports a conservative error envelope for the diffusion coefficient used in this calculation and even at the extreme, the slowest value of  $D$  within this range (i.e., the lowest value of  $D_0$  and the highest value of  $E_A$ ) is not consistent with a peak of metamorphism lasting as long as 50 Myr. Taken together, the experimental data and the measured gradient for  $\delta^{18}\text{O}$  (Fig. 6b) are most consistent with a thermal peak lasting less than 5 My. If these estimates of the diffusion rate of oxygen in garnet at 750  $^{\circ}\text{C}$  are correct, then the peak of regional metamorphism in the NE Adirondack Highlands was significantly faster than has previously been assumed. With increased understanding of the diffusion rate of oxygen in garnet and with further ion microprobe studies of single crystals, time and rate estimates based on oxygen diffusion profiles in garnet (and other minerals) will become more accurate than presently possible.

New technology and techniques used in the analysis of oxygen isotopes by ion microprobe have greatly improved the precision of the technique in the analysis of phases with limited solid solution. The use of a single garnet standard mounted in samples, regularly analyzed as a monitor for changes in instrumental conditions, provides similar precision in the analysis of garnets. The correction of instrumental bias due to cation composition in garnets can be done readily using 3 or more compositional standards in a separate standard mount. A correction scheme based on the grossular content of pyralispite garnets and the andradite content of ugrandite garnets brings the accuracy of analyses to the same order as analytical precision with a combined uncertainty of  $\pm 0.5$  to  $0.6\%$ , 2 S.D. Application of this approach to garnets will have widespread utility for estimation of thermal and fluid history during metamorphism.

## Acknowledgements

This research was begun while FZP was a post-doctoral fellow at the University of Wisconsin supported by (NSF-EAR 0509639). The authors thank Mike Spicuzza for laser fluorination analyses of  $\delta^{18}\text{O}$ , John Fournelle for assistance in electron microprobe analysis and SEM imaging, Brian Hess for sample preparation, and Bin Fu, Penny Lancaster, and Taka Ushikubo for their helpful conversations. Reviews by Ethan Baxter and Ryan Ickert substantially improved this paper. Dan Schulze, Daniel Vielzeuf, Matt Kohn, Lee Riciputi, John Eiler, Colin Graham, Steve Elphick, and John Craven provided the garnet samples. The acquisition of the SEM at Oberlin College used in this study was supported by NSF-CCLI (0087895). WiscSIMS is partly supported by NSF-EAR (0319230, 0744079), DOE (93ER14389).

## Appendix A. Supplementary data

Supplementary data associated with this article can be found, in the online version, at doi:10.1016/j.chemgeo.2009.11.001.

## References

- Afifi, A.M., Essene, E.J., 1988. Minfile: a microcomputer program for storage and manipulation of chemical data on minerals. *Am. Mineral.* 73, 446–448.
- Ague, J.J., Baxter, E.F., 2007. Brief thermal pulses during mountain building recorded by Sr diffusion in apatite and multicomponent diffusion in garnet. *Earth Planet. Sci. Lett.* 261, 500–516.
- Basu, A.R., Faggert, B.E., Sharma, M., 1988. Sm–Nd isotopic study of wollastonite skarn and garnet amphibolite metamorphism in the Adirondack Mountains, New York. *EOS* 69, 468.
- Bohlen, S.R., Valley, J.W., Essene, E.J., 1985. Metamorphism in the Adirondacks: I. Petrology, pressure and temperature. *J. Pet.* 26 (4), 971–992.
- Bowman, J.R., 1998. Stable-isotope systematics of skarns. In: Lentz, D.R. (Ed.), *Mineralized Intrusion-Related Skarn Systems*. Mineral. Assoc. Can. Short Course, vol. 26. Mineralogical Association of Canada, pp. 99–145.
- Cavosie, A.J., Valley, J.W., Wilde, S.A., EIMF, 2005. Magmatic  $\delta^{18}\text{O}$  in 4400–3900 Ma detrital zircons: a record of the alteration and recycling of crust in the Early Archean. *Earth Planet. Sci. Lett.* 235, 663–681.
- Clechenko, C.C., Valley, J.W., 2003. Oscillatory zoning in garnet from the Willsboro wollastonite skarn, Adirondack Mts, New York: a record of shallow hydrothermal processes preserved in a granulite facies terrane. *J. Metamorph. Geol.* 21, 771–784.
- Coghlan, R.A., 1990. Studies in diffusional transport: Grain boundary transport of oxygen in feldspars, diffusion of oxygen, strontium, and the REE's in garnet, and the thermal histories of granitic intrusions in south-central Maine using oxygen isotopes. PhD Thesis, Brown University, Providence, RI.
- Crank, J., 1975. *The mathematics of diffusion*. Oxford University Press, New York. 414 pp.
- Crowe, D.E., Riciputi, L.R., Bezenek, S., Ignatiev, A., 2001. Oxygen isotope and trace element zoning in hydrothermal garnets: windows into large-scale fluid-flow behavior. *Geology* 29, 479–482.
- Diella, V., Sani, A., Levy, D., Pavese, A., 2004. High-pressure synchrotron X-ray diffraction study of spessartine and uvarovite: a comparison between different equation of state models. *Am. Mineral.* 89, 371–376.
- Donovan, J.J., Kremser, D., Fournelle, J.H. (Eds.), 2007. *Probe for Windows User's Guide and Reference*, Enterprise Edition. 355 pp.
- Eiler, J.M., Graham, C.M., Valley, J.W., 1997. SIMS analysis of oxygen isotopes; matrix effects in complex minerals and glasses. *Chem. Geol.* 138, 221–244.
- Elsenheimer, D., Valley, J.W., 1993. Submillimeter scale zonation of  $\delta^{18}\text{O}$  in quartz and feldspar, Isle-of-Skye, Scotland. *Geochim. Cosmochim. Acta* 57, 3669–3676.
- Ford, F., 1987. Petrology and geochemistry of xenoliths from the Blaauwbosch kimberlite pipe, R.S.A., Undergraduate Thesis, University of Toronto, Toronto.
- Garlick, G.D., Macgregor, I.D., Vogel, D.E., 1971. Oxygen isotope ratios in eclogites from kimberlites. *Science* 172, 1025–1027.
- Gnaser, H., 2008. Isotopic fractionation of sputtered anions:  $\text{C}^-$  and  $\text{C}_2^-$ . *Nucl. Instrum. Methods Phys. Res., Sect. B* 266, 37–43.
- Hervig, R.L., Williams, P., Thomas, R.M., Schauer, S.N., Steele, I.M., 1992. Microanalysis of oxygen isotopes in insulators by secondary ion mass spectrometry. *Int. J. Mass Spectrom. Ion Process.* 120, 45–63.
- Huberty, J.M., Kita, N.T., Heck, P.R., Kozdon, R., Fournelle, J.H., Xu, H., Valley, J.W., 2009. Crystal orientation effects on bias of  $\delta^{18}\text{O}$  in magnetite by SIMS. *Goldschmidt Conference, Geochim. Cosmochim. Acta*, vol. 73:135, p. A562.
- Jamtveit, B., Hervig, R.L., 1994. Constraints on transport and kinetics in hydrothermal systems from zoned garnet crystals. *Science* 263, 505–508.
- Jamtveit, B., Wogelius, R.A., Fraser, D.G., 1993. Zonation patterns of skarn garnets – records of hydrothermal system evolution. *Geology* 21, 113–116.
- Kelly, J.L., Fu, B., Kita, N.T., Valley, J.W., 2007. Optically continuous silcrete quartz cements of the St. Peter Sandstone: high precision oxygen isotope analysis by ion microprobe. *Geochim. Cosmochim. Acta* 71, 3812–3832.
- Kita, N.T., Ushikubo, T., Fu, B., Valley, J.W., 2009. High precision SIMS oxygen isotope analyses and the effect of sample topography. *Chem. Geol.* 264, 43–57.
- Kohn, M.J., Valley, J.W., 1994. Oxygen isotope constraints on metamorphic fluid flow, Townshend Dam, Vermont, USA. *Geochim. Cosmochim. Acta* 58, 5551–5566.
- Kohn, M.J., Valley, J.W., 1998. Effects of cation substitutions in garnet and pyroxene on equilibrium oxygen isotope fractionations. *J. Metamorph. Geol.* 16, 625–639.
- Kohn, M.J., Valley, J.W., Elsenheimer, D., Spicuzza, M.J., 1993. Isotope zoning in garnet and staurolite; evidence for closed-system mineral growth during regional metamorphism. *Am. Mineral.* 78, 988–1001.
- Kohn, M.J., Spear, F.S., Valley, J.W., 1997. Dehydration-melting and fluid recycling during metamorphism: Rangeley Formation, New Hampshire, USA. *J. Petrol.* 38, 1255–1277.
- Lancaster, P.J., Fu, B., Page, F.Z., Kita, N.T., Bickford, M.E., Hill, B.M., McLelland, J.M., Valley, J.W., 2009. Genesis of metapelitic migmatites in the Adirondack Mts., New York. *J. Metamorph. Geol.* 27, 41–54.
- MacGregor, I.D., Manton, W.I., 1986. Roberts Victor eclogites: ancient oceanic crust. *J. Geophys. Res.* 91, 14,063–14,079.
- Martin, L., Duchêne, S., Deloule, E., Vanderhaeghe, O., 2006. The isotopic composition of zircon and garnet: a record of the metamorphic history of Naxos, Greece. *Lithos* 87, 174–192.
- McLelland, J., Hamilton, M., Selleck, B., McLelland, J., Walker, D., Orrell, S., 2001. Zircon U–Pb geochronology of the Ottawa Orogeny, Adirondack Highlands, New York: regional and tectonic implications. *Precambrian Res.* 109, 39–72.
- McLelland, J.M., Bickford, M.E., Hill, B.M., Clechenko, C.C., Valley, J.W., Hamilton, M.A., 2004. Direct dating of Adirondack Massif anorthosite by U–Pb SHRIMP analysis of igneous zircon; implications for AMCG complexes. *Geol. Soc. Am. Bull.* 116 (11–12), 1299–1317.
- Mezger, K., Rawnsley, C., Bohlen, S.R., Hanson, G.N., 1991. U–Pb garnet, sphene, monazite, and rutile ages: implications for the duration of high grade metamorphism and cooling histories, Adirondack Mts., New York. *J. Geol.* 99, 415–428.
- Novak, G., Gibbs, G.V., 1971. The crystal chemistry of silicate garnets. *Am. Mineral.* 56, 791–825.
- Page, F.Z., Ushikubo, T., Kita, N.T., Riciputi, L.R., Valley, J.W., 2007. High-precision oxygen isotope analysis of picogram samples reveals 2  $\mu\text{m}$  gradients and slow diffusion in zircon. *Am. Mineral.* 92, 1772–1775.
- Peck, W.H., Valley, J.W., 2004. Quartz–garnet isotope thermometry in the south Adirondack Highlands (Grenville Province, New York). *J. Metamorph. Geol.* 22, 763–773.
- Riciputi, L.R., Paterson, B.A., 1994. High spatial-resolution measurement of O isotope ratios in silicates and carbonates by ion microprobe. *Am. Mineral.* 79, 1227–1230.
- Riciputi, L.R., Paterson, B.A., Ripperdan, R.L., 1998. Measurement of light stable isotope ratios by SIMS: matrix effects for oxygen, carbon, and sulfur isotopes in minerals. *Int. J. Mass Spectrom.* 178, 81–112.
- Robie, R.A., Hemingway, B.S., 1995. Thermodynamic properties of minerals and related substances at 298.15 K and 1 bar ( $10^5$  Pascals) pressure and at higher temperatures. B 2131, U. S. Geological Survey, Reston.
- Schulze, D.J., Valley, J.W., Spicuzza, M.J., 2003. The oxygen isotope composition of mantle eclogites. 8th International Kimberlite Conference, Victoria, B.C.
- Shimizu, N., Hart, S.R., 1982. Isotope fractionation in secondary ion mass-spectrometry. *J. Appl. Phys.* 53, 1303–1311.
- Skelton, A., Annersten, H., Valley, J., 2002.  $\delta^{18}\text{O}$  and yttrium zoning in garnet: time markers for fluid flow? *J. Metamorph. Geol.* 20, 457–466.
- Taylor, B.E., O'Neil, J.R., 1977. Stable isotope studies of metasomatic Ca–Fe–Al–Si skarns and associated metamorphic and igneous rocks, Osgood Mountains, Nevada. *Contrib. Mineral. Petrol.* 63, 1–49.
- Valley, J.W., 1985. Polymetamorphism in the Adirondacks: wollastonite at contacts of shallowly intruded anorthosite. In: Tobi, A.C., Touret Jacques, L.R. (Eds.), *The Deep Proterozoic Crust in the North Atlantic Provinces*. Reidel, Dordrecht, pp. 217–236.
- Valley, J.W., 1986. Stable isotope geochemistry of metamorphic rocks. In: Valley, J.W., Taylor, H.P., O'Neil, J.R. (Eds.), *Stable isotopes in high temperature geological processes*. Rev. Mineral., vol. 16, pp. 445–489.
- Valley, J.W., Graham, C.M., 1991. Ion microprobe analysis of oxygen isotope ratios in granulite facies magnetites; diffusive exchange as a guide to cooling history. *Contrib. Mineral. Petrol.* 109, 38–52.
- Valley, J.W., Kita, N.T., 2009. *In situ* oxygen isotope geochemistry by ion microprobe. In: Fayek, M. (Ed.), *GAC/MAC Short Course: Secondary Ion Mass Spectrometry in the Earth and Planetary Sciences*, vol. 41, pp. 19–63.
- Valley, J.W., O'Neil, J.R., 1982. Oxygen isotope evidence for shallow emplacement of Adirondack anorthosite. *Nature* 300, 497–500.
- Valley, J.W., Bohlen, S.R., Essene, E.J., Lamb, W., 1990. Metamorphism in the Adirondacks: II, The role of fluids. *J. Petrol.* 31 (3), 555–596.
- Valley, J.W., Kitchen, N., Kohn, M.J., Niendorf, C.R., Spicuzza, M.J., 1995. UWG-2, a garnet standard for oxygen isotope ratios: strategies for high precision and accuracy with laser heating. *Geochim. Cosmochim. Acta* 59, 5223–5231.
- Vielzeuf, D., Champenois, M., Valley, J.W., Brunet, F., Devidal, J.L., 2005a. SIMS analyses of oxygen isotopes: matrix effects in Fe–Mg–Ca garnets. *Chem. Geol.* 223, 208–226.
- Vielzeuf, D., Veschambre, M., Brunet, F., 2005b. Oxygen isotope heterogeneities and diffusional profiles in composite metamorphic/magmatic garnets from the Pyrenees. *Am. Mineral.* 90, 463–472.
- Yardley, B.W.D., Rochelle, C.A., Barnicoat, A.C., Lloyd, G.E., 1991. Oscillatory zoning in metamorphic minerals – an indicator of infiltration metasomatism. *Mineral. Mag.* 55, 357–365.